PHYSICAL REVIEW B **72**, 064104 (2005)

Intermediate ferroelectric orthorhombic and monoclinic M_B phases in [110] electric-field-cooled $Pb(Mg_{1/3}Nb_{2/3})O_3$–30%$PbTiO_3$ crystals

Hu Cao, Feiming Bai, Naigang Wang, Jiefang Li, and D. Viehland
Department of Materials Science and Engineering, Virginia Tech, Blacksburg, Virginia 24061, USA

Guangyong Xu and Gen Shirane
Physics Department, Brookhaven National Laboratory, Upton, New York 11973, USA
(Received 1 April 2005; published 5 August 2005)

Structural phase transformations of [110] electric-field-cooled $Pb(Mg_{1/3}Nb_{2/3})O_3$-30%$PbTiO_3$ (PMN-30%PT) crystals have been performed by x-ray diffraction. A phase sequence of cubic (C)→ tetragonal (T) → orthorhombic (O)→ monoclinic (M_B) was found on field cooling (FC); and a rhombohedral (R)→M_B →O sequence was observed with increasing field, beginning from the zero-field-cooled condition at room temperature. The application of the [110] electric field induced a dramatic change in the phase sequence in the FC condition, compared to the corresponding data for PMN-30%PT crystals in a [001] field, which shows that the phase sequence in the FC condition is altered by the crystallographic direction along which a modest electric field (E) is applied. Only when E is applied along [110] are intermediate O and M_B phases observed.

DOI: 10.1103/PhysRevB.72.064104 PACS number(s): 61.10.Nz, 77.84.Dy, 77.80.Bh

I. INTRODUCTION

Relaxor ferroelectric-based morphotropic phase-boundary (MPB) crystals, such as $(1-x)Pb(Mg_{1/3}Nb_{2/3}O_3)$-$xPbTiO_3$ (PMN-x%PT) and $(1-x)Pb(Zn_{1/3}Nb_{2/3}O_3)$-$xPbTiO_3$ (PZN-x%PT),[1] have attracted much interest as high-performance piezoelectric actuator and transducer materials. For example, (001)-oriented PMN-33%PT crystals, which lie at the MPB, have the highest piezoelectric ($d_{33}\sim 2500$ pC/N) and electromechanical coupling ($k_{33}\sim 94\%$) (Ref. [2])coefficients. Following conventional thought,[3] the MPB is supposed to be a vertical boundary between ferroelectric rhombohedral (R) and tetragonal (T) phases.

Park and Shrout[1,4] conjectured that the high-electromechanical properties of PMN-x%PT and PZN-x%PT was due to a $R\rightarrow T$ phase transition induced by an applied electric field (E). More recently, an important breakthrough in understanding the structural origin of the high-electromechanical properties of MPB compositions has been made: the discovery of ferroelectric monoclinic (M) phases bridging the R and T ones, which was reported for $Pb(Zr_xTi_{1-x})O_3$.[5–7] Subsequently, x-ray diffraction (XRD) and neutron diffraction experiments have shown the existence of various ferroelectric M phases in oriented PZN-x%PT (Refs. 8–12) and PMN-x%PT (Refs. 12–15) crystals, including M_A and M_C. Recent neutron diffraction studies of the effect of an applied E along [001] on the phase stability of PZN-8%PT by Ohwada *et al.*[11] have shown a $R\rightarrow M_A\rightarrow M_C\rightarrow T$ phase sequence with increasing E at 350 K beginning from the zero-field-cooled (ZFC) condition, and a $C\rightarrow T\rightarrow M_C$ sequence in the field-cooled (FC) condition. Similar M_A and M_C phases have also been reported in PMN-x%PT.[12–15] A recent study by Bai *et al.*[15] established that PMN-30%PT has a $C\rightarrow T\rightarrow M_C\rightarrow M_A$ sequence in the FC condition with the application of an electric field along the [001] direction, and a $R\rightarrow M_A\rightarrow M_C\rightarrow T$ sequence with increasing E beginning from the ZFC. The findings of prior diffraction studies of phase stability in [001] electric-field-cooled PMN-30%PT crystals are summarized in Fig. 1(a).

The monoclinic symmetry allows the polarization vector to be unconstrained within a plane, rather than constricted to a particular crystallographic axis as for the higher symmetry R, T, or orthorhombic (O) phases. According to the polarization rotation theory,[16] the high-electromechanical properties of ferroelectric monoclinic phases are due to the rotation

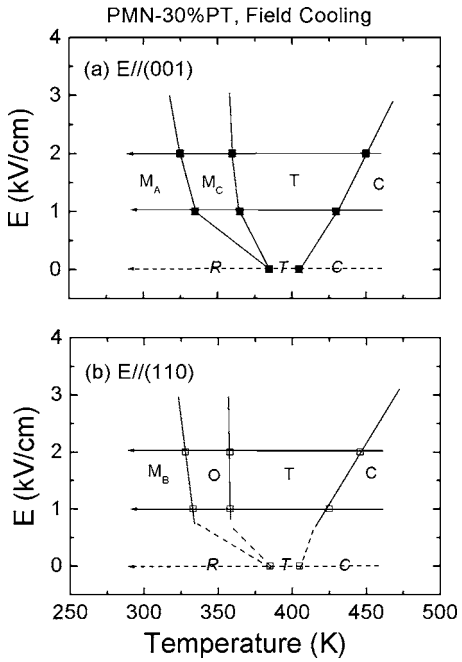

FIG. 1. E-T phase diagram. Top panel (a) is PMN-30%PT in the FC condition by Bai (Ref. 15) with E along [001]; bottom panel (b) is PMN-30%PT in the FC condition with E along [110]. Arrows indicate the sequence of phase transition in the FC condition. Dotted lines indicate the ZFC condition, and solid lines indicate the FC condition.

of the polarization vector within the symmetry-allowed plane. Vanderbilt and Cohen predicted the stability ranges of monoclinic M_A and M_C phases using a thermodynamic approach;[17] in addition, they predicted a possible narrow-stability range of a M_B phase, intermediate between the R and M_C phases. Prior structural studies of PMN-x%PT and PZN-x%PT have only been performed under an E applied along the [001] direction—however, this is not an inherent restriction, as polarization rotation could occur in either direction in the permissible planes. For $BaTiO_3$, structural studies have been performed by Wada *et al.*[18] under an E applied along the [111] direction, where a $T \rightarrow O \rightarrow R$ phase sequence was observed with increasing E at 300 K, and where optical birefringence indicated the presence of bridging M phases. Dielectric property studies of PMN-33%PT crystals with E along [110] have been reported by Lu *et al.*,[19] who reported an intermittently present metastable phase over a narrow temperature range sandwiched between M_C and M_A phases in the FC condition. Polarized-light microscopy (PLM) indicated that this evasive phase was a single-domain orthorhombic one.[20] In addition, the P-E and ε-E behaviors of ZFC PMN-30%PT crystals with E along [110] have been reported by Viehland and Li,[21] who conjectured a field-induced O phase at room temperature via a monoclinic M_B phase. However, structural studies have not yet established this to be the case, nor has the phase sequence in [110] FC crystals yet been identified.

In this investigation, we have focused on establishing the structural transformation sequence of PMN-30%PT crystals with E along [110], and on determining how this sequence compares to that of the corresponding [001] FC sequence. Our results suggest that the phase sequences in an FC process with the electric field along different crystallographic orientations are distinctively different, as shown in Fig. 1. XRD studies on PMN-30%PT under a [110] electric field have unambiguously shown a phase sequence of $C \rightarrow T \rightarrow O \rightarrow M_B$ for [110] FC PMN-30%PT, and a sequence of $R \rightarrow M_B \rightarrow O$ with increasing field beginning from the ZFC condition at room temperature.

II. EXPERIMENTAL PROCEDURE

Single crystals of PMN-30%PT with dimensions of $3 \times 3 \times 3$ mm^3 were obtained from HC Materials (Urbana, IL), and were grown by a top-seeded modified Bridgman method. The cubes were oriented along the pseudocubic $(1\bar{1}1)/(110)/(\bar{1}12)$ planes, and were polished to 0.25 μm. Gold electrodes were deposited on one pair of opposite (110) faces of the cube by sputtering. Temperature-dependent dielectric-constant measurements were performed using a multiple-frequency *LCR* meter (HP 4284A) under various E.

The XRD studies were performed using a Philips MPD high-resolution system equipped with a two-bounce hybrid monochromator, an open three-circle Eulerian cradle, and a doomed hot-stage. A Ge (220)-cut crystal was used as an analyzer, which had an angular resolution of 0.0068°. The x-ray wavelength was that of Cu $K\alpha = 1.5406$ Å, and the x-ray generator operated at 45 kV and 40 mA. The penetration depth in the samples was on the order of 10 μm. The

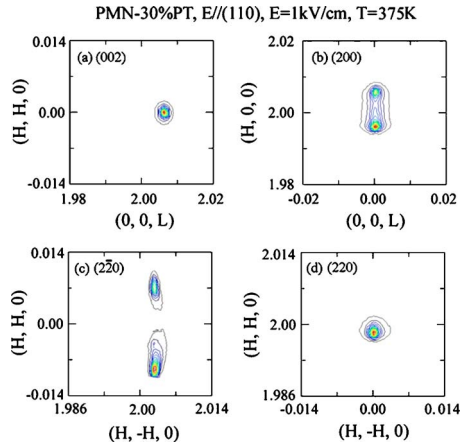

FIG. 2. (Color online) Mesh scans of (002), (200), (2$\bar{2}$0), and (220) of PMN-30%PT with $E = 1$ kV/cm applied along [110] at 375 K in the FC condition.

domain structure for PMN-30%PT under a [110] electric field can become quite complicated. In our diffraction studies, we have performed mesh scans around the (002) Bragg reflection in the (H,H,L) zone, defined by the [110] and [001] vectors; the (220) and (2$\bar{2}$0) reflections in the scattering zone, defined by the [110] and [1$\bar{1}$0] vectors; and (200) in the (H,O,L) zone, defined by the [100] and [001] vectors. Each measurement cycle was begun by heating up to 550 K to depole the crystal, and measurements were subsequently taken on cooling. At 525 K, the lattice constant of PMN-30%PT was $a = 4.027$ Å; correspondingly, the reciprocal lattice unit (or 1 rlu) was $a^* = 2\pi/a = 1.560$ Å^{-1}. All mesh scans of PMN-30%PT with E along [110] shown in this study were plotted in reference to this reciprocal unit.

III. RESULTS

A. Field-cooled condition

1. Structural determination of different phases of various phase fields

To determine the effect of E on the phase sequence, we measured changes in mesh scans on field-cooling under $E = 1$ and 2 kV/cm. At 450 K under $E = 1$ kV/cm (data not shown), the (002) and (220) mesh scans did not exhibit splitting, and it was found that $c = a$. Thus it is clear that the lattice is cubic. As the temperature was decreased to 420 K, the (002) reflection shifted toward slightly shorter wave vectors, and a splitting along the longitudinal direction was found around the (200) reflection, indicating a transition to the T phase. The signature of the T phase became more pronounced with decreasing temperature.

An electric field of 1 kV/cm was then applied along the [110] direction. Figures 2(a)–2(d) show mesh scans taken around the (002), (200), (2$\bar{2}$0), and (220) for PMN-30%PT when the sample was cooled in the field to 375 K, respectively. The (002) reflection [see Fig. 2(a)] had only a single sharp peak. The lattice constant extracted from the (002) reflection was 4.0140 Å. However, the (200) reflection [see

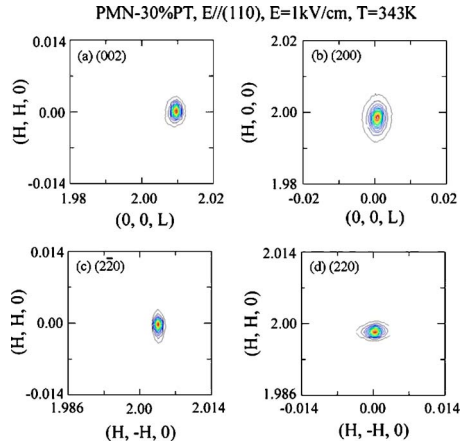

FIG. 3. (Color online) Mesh scans of (002), (200), (2$\bar{2}$0), and (220) of PMN-30%PT with $E=1$ kV/cm applied along [110] at 325 K in the FC condition.

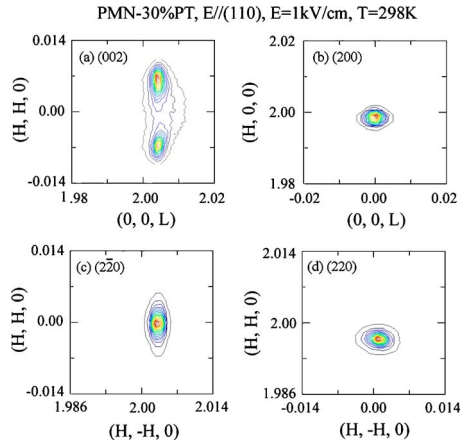

FIG. 4. (Color online) Mesh scans of (002), (200),(2$\bar{2}$0), and (220) of PMN-30%PT with $E=1$ kV/cm applied along [110] at 298 K in the FC condition.

Fig. 2(b)] splits into two peaks along the longitudinal direction, from which the lattice parameters can be determined to be $a=4.0142$ Å and $c=4.0329$ Å, which are quite consistent with those found around the other zones in Fig. 2. These results for PMN-30%PT with E along [110] reveal a tetragonal ferroelectric phase with twinned a and b domains along [200] or [020]. In addition, the (2$\bar{2}$0) mesh scan [see Fig. 2(c)] splits into two peaks only along the transverse direction, whereas the (220) scan [see Fig. 2(d)] has only a single peak. This indicates that the [110] field fixes the [110] crystallographic orientation, and that twinned a and b domains in the (001) plane are present in the [2$\bar{2}$0] scan along the transverse direction. Thus, it is evident that PMN-30%PT has a tetragonal lattice, in which the polarizations are constrained to [100] and [010] directions for a and b domains.

As the temperature decreased, the longitudinal splitting in the (200) mesh scan disappeared near 358 K, indicating another phase transformation. Figures 3(a)–3(d) show mesh scans taken about (002), (200), (2$\bar{2}$0), and (220) within this phase field at 343 K. Interestingly, only a single domain in each of these mesh scans was observed, indicating the presence of a well-developed single domain throughout the entire crystal. The structure of this phase was determined to be orthorhombic, where the polarization is fixed to the [110] direction. The lattice parameters of this orthorhombic phase were determined from the mesh scans to be $a_0=5.6924$ Å, $b_0=5.6812$ Å, and $c_0=4.0070$ Å, where a_0 was extracted from the (220) reflection, b_0 from the (2 $\bar{2}$ 0) one, and c_0 from the (002) one. This unit cell is a doubled one, consisting of two M_C simple cells, as previously reported for orthorhombic $BaTiO_3$.[22]

Upon further decrease of the temperature to ~333 K, the (002) mesh scan was found to split only along the transverse direction, revealing yet another phase transition. Figures 4(a)–4(d) show (002), (200), (2$\bar{2}$0), and (220) scans taken for $E=1$ kV/cm at 298 K. The (002) reflection [see Fig. 4(a)] can be seen to split into two peaks with the same wave-vector length, whereas the other three mesh scans remained as a single peak. This is a signature of the monoclinic M_A/M_B phase. We then determined the lattice parameters (by extraction from the mesh scans in Fig. 4), to be $c_M=4.0204$, $a_M/\sqrt{2}=4.0280$ Å, and $b_M/\sqrt{2}=4.0181$ Å; where a_M and b_M were derived from the (220) and (2$\bar{2}$0) reflections, and c_M from the (002) reflection. Our results show that on field cooling below ~333 K, a [110] field cooling can no longer sustain a single-domain O phase whose polarization is fixed to the [110] direction; rather, a transition to a polydomain monoclinic phase occurs. The unit cells of both the M_A and M_B phases are doubled with respect to the primitive pseudocubic one, where the polarization lies in the (1$\bar{1}$0) crystallographic plane. Although both the M_A and M_B phases belong to the c_M space group, there is a difference between their polarizations: for M_A, $P_x=P_y<P_z$, whereas for M_B, $P_x=P_y>P_z$. The fact $a_M/\sqrt{2}>c_M$ confirms that this monoclinic phase is the M_B one. This is the first direct confirmation of the presence of the M_B phase in the transformational sequence of either PMN-x%PT or PZN-x%PT single crystals. It is relevant to note our prior reports of property data that indicate a $R\rightarrow M_B\rightarrow O$ phase transformational sequence in the ZFC condition[21] and equally relevant to note that it is consistent with the thermodynamic theory of Vanderbilt and Cohen[17] that allows for this sequence.

2. Lattice parameters and dielectric behavior in the FC condition

The lattice parameters of [110] electric-field-cooled PMN-30%PT at $E=1$ kV/cm are plotted as a function of temperature in Fig. 5. The lattice parameter a_C continuously decreases from 525 K on cooling. At 428 K, the value of a_C began to gradually increase, indicating the formation of a small volume fraction of tetragonal phase. Near 415 K, a splitting of the lattice parameter into a_T and c_T was observed, and the crystal was completely transformed into the T phase, where a_T was derived from the (002) reflection, whereas c_T was derived from the (200) one. Here, one thing should be mentioned. The [110] field-cooled PMN-30%PT was a little different than the [001] field-cooled one, not only with regards to the domain configurations, but also with respect to the derivation of the lattice parameters. For example, in the T

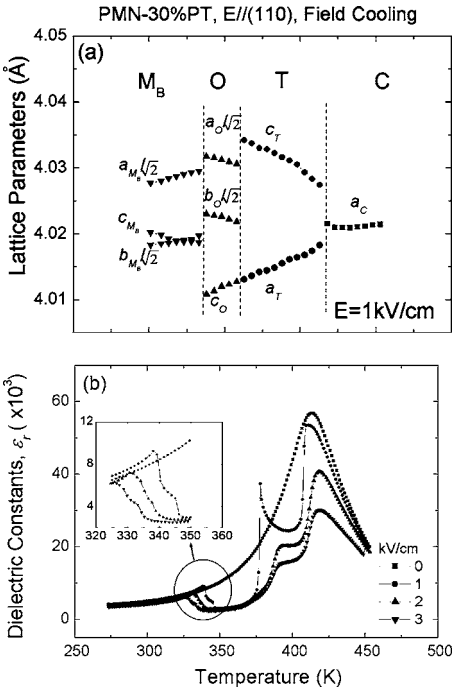

FIG. 5. Temperature dependence of (a) lattice constants for PMN-30%PT with $E=1$ kV/cm along [110], in which the lattice parameters $a_O/\sqrt{2}, b_O/\sqrt{2}$, and c_O and c_{M_B}, $a_{M_B}/\sqrt{2}$, and $b_{M_B}/\sqrt{2}$ are plotted, and (b) dielectric behavior under various levels of electric field at $f=1$ kHz in the FC condition.

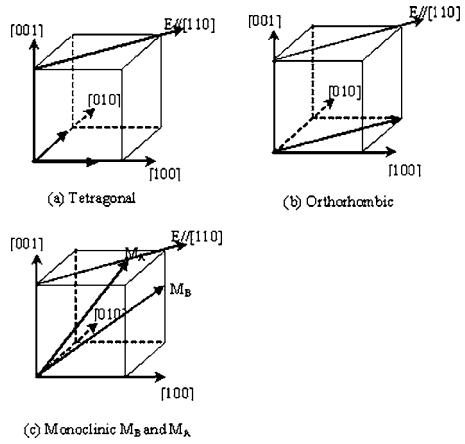

FIG. 6. Schematic of tetragonal, orthorhombic, and monoclinic M_C phases in PMN-30% PT with E along [110]. Arrows indicate the polar vector. Panel (a) is twin domains developed in the tetragonal phase; only two polarizations are constrained within the (001) plane. Panel (b) shows the single domain developed in the orthorhombic phase. Panel (c) indicates the domains developed in the M_B/M_A phase, in which the polarization vectors are constrained with the (110) plane.

phase, a_T was derived from the (200) reflection and c_T from The (002) reflection for [001] field-cooled PMN-30%PT. The $C\rightarrow T$ boundary shifted toward higher temperatures under a field of $E=1$ kV/cm, relative to the ZFC condition. As the temperature was further decreased, subsequent phase transitions were observed. Between 358 K and 333 K, an orthorhombic phase was found with lattice parameters of c_O, a_O, and b_O. It is worth noting that the values of c_O and a_T, both determined from the (002) reflection, were continuous at the $T\rightarrow O$ transformation. The orthorhombic unit cell is a doubled one; thus, the two lattice parameters, a_O and b_O, are double the size of the corresponding monoclinic M_C unit cell. The values of $a_O/\sqrt{2}$ in Fig. 5(a) exhibit a sharp decrease at the $T\rightarrow O$ transformation relative to c_T, whereas the value of $b_O/\sqrt{2}$ exhibits a sharp increase during the transition relative to a_T. On further cooling below 333 K, a transformation to a monoclinic M_B phase was observed with three lattice values, c_{M_B}, $b_{M_B}/\sqrt{2}$, and $a_{M_B}/\sqrt{2}$. At the $O\rightarrow M_B$ transformation, the values of $a_{M_B}/\sqrt{2}$ and $b_{M_B}/\sqrt{2}$ exhibited a sharp decrease, whereas c_{M_B} had a sharp increase.

The dielectric behavior of [110] electric-field-cooled PMN-30%PT is shown in Fig. 5(b). A platelike sample (0.7 mm thickness) was polished from the original cubic-shape crystal used in the XRD studies. The results are consistent with the transformational sequence of $C\rightarrow T\rightarrow O\rightarrow M_B$ in the FC condition for various field levels. First, no significant shift of the value of the temperature of the dielectric maximum ($T_{\max}$) was observed at the $C\rightarrow T$ transformation with increasing E. It is relevant to note that the $C\rightarrow T$ boundary as determined by $T_{\max}$ did not shift with E, unlike that determined from the XRD data. We are currently investigating this difference, which was not the aim of the present work. The results of Fig. 5(b) also show subsequent lower-temperature phase transitions, corresponding to the $T\rightarrow O$ and $O\rightarrow M_B$ transitions observed with the lattice parameter changes in Fig. 5(a). The value of the dielectric constant was relatively high in all phase fields, except in the single-domain orthorhombic region, in which the polar vector coincides with the direction of [110] applied E.

3. Summary of domain configurations in [110] electric-field-cooled T, O, and M_B phases

Figure 6 conceptually summarizes the domain configurations of the T, O, and $M_{\mathbf{B}}$ phases, in which an E has been applied along the [110] direction. In a ferroelectric T phase, six equivalent variants are permissible along the [100] direction. However, only two of these six are favored by applying an E along [110]: [100] and [010]. In the T phase of [110] electric-field-cooled PMN-30%PT, the [110] axis was fixed by the [110] field, and accordingly twinned a and b domains were found along the [100] and [010] directions, as shown in Fig. 6(a).

Figure 6(c) illustrates the single-domain orthorhombic state that is established throughout the crystal by [110] field cooling. Within this single domain, the polarization is fixed to only the [110] orthorhombic variant. There is no monoclinic tilting of this O variant away from the [110] direction. This unit cell is a doubled one, formed by perfectly adjusting two M_C simple cells.

The domain configurations of monoclinic phases are quite complicated; however, once an E is applied, a much simpler situation prevails.[8] For example, in the case of [001] electric-field-cooled PMN-30%PT (Ref. 15) or PZN-8%PT,[11] the field fixes the c axis to lie along the pseudocubic [001] direction; thus, there are only two b domains related by a 90°

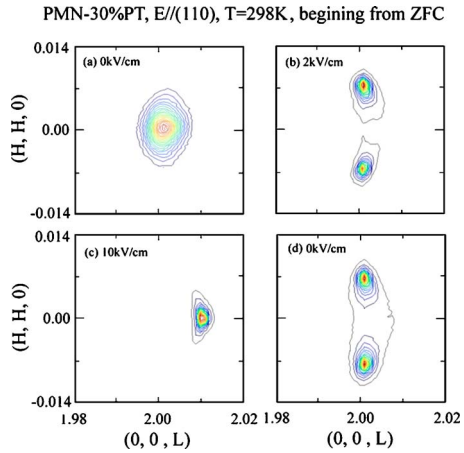

FIG. 7. (Color online) (002) mesh scans at 298 K with increasing fields of (a) 0 kV/cm, (b) 2 kV/cm, (c) 10 kV/cm, and (d) after removal of field in the poled condition.

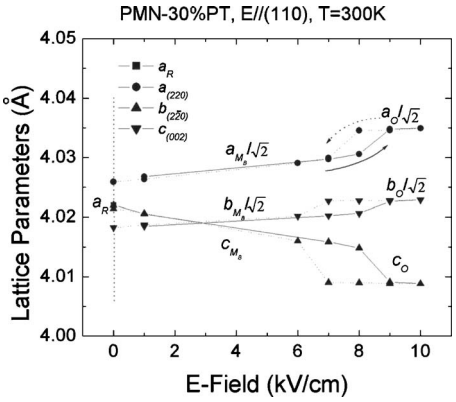

FIG. 8. Electric-field dependence of the lattice parameters at 298 K beginning from the ZFC condition, where lattice parameters $a_{(220)}/\sqrt{2}$, $b_{(2\bar{2}0)}/\sqrt{2}$, and $c_{(002)}$ are plotted. Solid lines represent data obtained on field increasing; dotted lines represent data obtained on field decreasing. At $E=0$ kV/cm, $c_{(002)}=a_R$, and once E is applied, $a_{(220)}/\sqrt{2}$, $b_{(2\bar{2}0)}/\sqrt{2}$, and $c_{(002)}$ correspond to $a_{M_B}/\sqrt{2}$, $b_{M_B}/\sqrt{2}$, and c_{M_B} in the M_B phase and to $a_O/\sqrt{2}$, $b_O/\sqrt{2}$, and c_O in the O phase, respectively.

rotation around the c axis, each of which has two a domains. These are M_C (a axis along [100]) and M_A (a axis along [110]) domain configurations previously reported for PMN-30%PT (Ref. 15) and PZN-8%PT.[11] However, [110] field cooling may result in slightly more complicated domain configurations, as an E does not fix the c axis to be along the [001] direction; rather, [110] field cooling fixes the [110] direction and forces the polarization as close as possible to the [110], as illustrated in Fig. 6(c). However, in the monoclinic phase of [110] field-cooled PMN-30%PT, the polarization is rotated away from the orthorhombic within the $(1\bar{1}0)$ plane, pointing toward the [001]. This domain configuration is that of the monoclinic M_B phase, since $P_x=P_y>P_z$ and $a_{M_B}/\sqrt{2}>c_{M_B}$. In this case, two polarizations were constrained to the $(1\bar{1}0)$ plane, consistent with a single peak in the (220) mesh scan and two domains in the (002) mesh scan.

B. Phase stability with increasing E, beginning from ZFC

The field dependence of the lattice parameters was then investigated at room temperature, beginning from the ZFC condition. The crystal was first heated to 525 K, and subsequently cooled under zero field. The (002) and (220) XRD mesh scans were obtained at various dc biases. Figures 7(a)–7(d) show the (002) scans for the field sequence of $E=0$ kV/cm, 2 kV/cm, 10 kV/cm, and $E=0$ kV/cm (i.e., after removal of E) at 298 K, respectively. For $E=0$ kV/cm, only a single broad peak was found in the (002) scan, although a longitudinal splitting was observed in the (220) scan (data not shown). The results show that the R phase is stable in the ZFC condition, with a lattice parameter of $a_R=4.0220$ Å. Upon applying a field of 1 kV/cm, a peak splitting was found to develop along the transverse direction in the (002) reflection, whereas the (220) scan only possessed a single peak (data not shown). These features are signatures of the monoclinic M_B/M_A phase. The lattice parameters c_{M_B} and a_{M_B}, extracted from the (002) and (220) reflections, show that $a_{M_B}/\sqrt{2}>c_{M_B}$. Thus, we can conclude that the phase transformational sequence beginning from the ZFC condition is $R\rightarrow M_B\rightarrow O$ with increasing E, with the $R\rightarrow M_B$ transition at $E<1$ kV/cm and the $M_B\rightarrow O$ one near $E=10$ kV/cm.

Figure 8 shows the electric-field dependence of the lattice parameters at 298 K. With increasing E to 8 kV/cm, the value of $a_{M_B}/\sqrt{2}$ and $b_{M_B}/\sqrt{2}$ can be seen to continuously increase, exhibiting a sharp increment at 9 kV/cm, whereas the value of C_{M_B} shows a gradual decrease and has a sharp decrease at 9 kV/cm, at which point a single-domain O phase is induced. Comparisons with the FC results in Fig. 5(a) indicate that the crystal undergoes an abrupt transition to the O phase near 9 kV/cm. It is also important to compare these results to recent studies of PMN-30%PT with E along [110] crystals by Li and Viehland,[21] which indicated an induced phase transformation near this same field in the ZFC condition. It is relevant to note that an hysteretic P-E behavior was observed, whose remnant polarization was ~ 0.24 C/m^2 (or $P_s/\sqrt{3}$) and whose value at the induced transition was ~ 0.3 C/m^2 (or $P_s/\sqrt{2}$). It appears that the polarization can nearly continuously rotate within the (110) plane of the M_B phase, from near the [111] direction to being in coincidence with the [110].

With decreasing electric field between 9 kV/cm and 6 kV/cm, the lattice parameters revealed hysteresis of the induced $M_B\rightarrow O$ transformation. For $E<6$ kV/cm, the orthorhombic phase did not remain stable, but rather an M_B phase was recovered. In addition, for $E<6$ kV/cm, the lattice parameters were equivalent between field-increasing and field-decreasing sweeps. Upon removal of E, only a single domain was observed in the (220) scan, although a splitting along [220] was found in the (002) scan. We determined the monoclinic lattice parameters after removal of E and found that $a_{M_B}/\sqrt{2}>C_{M_B}$. These results show that the M_B phase is the ground-state condition for poled (110) crystals.

IV. SUMMARY

We summarize our findings in an E-T diagram concerning the ferroelectric stability of [110] oriented PMN-30%PT crystals in a [110] field, as shown in Fig. 1(b). For comparison, a corresponding E-T diagram for the [001] field was given in Fig. 1(a). The $C \rightarrow T$ boundaries in the FC condition were also nearly identical for both orientations, shifting by nearly the same degree with increasing E over the range studied. Significant difference between the [110] and [001] fields only became unambiguous on field cooling to lower temperatures. For an E applied along the [110] direction, the sequence was found to be $C \rightarrow T \rightarrow O \rightarrow M_B$, whereas for an E applied along the [001] direction, the sequence was $C \rightarrow T \rightarrow M_C \rightarrow M_A$. In Fig. 1(b), an intermediate O phase exists only when E is applied along the [110] direction, which constrains the polarization within the pseudocubic $(1\bar{1}0)$ plane and the $T \rightarrow O$ boundary can be seen to be quite vertical for $E < 3$ kV/cm. A transition occurred with decreasing temperature in the FC condition, where the $O \rightarrow M_B$ boundary shifted toward lower temperature with increasing E at a rate of 5 Kcm/kV. Beginning from the ZFC condition at room temperature, the phase-transformational sequence of $R \rightarrow M_B \rightarrow O$ was observed with increasing E. Upon removal of the electric field, the crystal shows M_B as the ground state.

Our results clearly demonstrate (i) the presence of intermediate ferroelectric orthorhombic and monoclinic M_B phases in PMN-x%PT (or PZN-x%PT) crystals; (ii) a phase sequence of $C \rightarrow T \rightarrow O \rightarrow M_B$ for [110] field-cooled PMN-30%PT, and a sequence of $R \rightarrow M_B \rightarrow O$ with increasing E along [110], beginning from the ZFC condition at room temperature.

ACKNOWLEDGMENTS

We would like to gratefully acknowledge financial support from the Office of Naval Research under Grant Nos. N000140210340, N000140210126, and MURI N0000140110761; U.S. Department of Energy under Contract No. DE-AC02-98CH10886. We would like to thank HC Materials for providing the single crystals used in this study. In particular, we would also like to acknowledge the tremendous help that Gen. Shirane has provided to us.

[1] S.-E. Park and T. R. Shrout, J. Appl. Phys. **82**, 1804 (1997).
[2] H. S. Luo, G. S. Xu, H. Q. Xu, P. C. Wang, and Z. W. Yin, Jpn. J. Appl. Phys., Part 1 **39**, 5581 (2000).
[3] B. Jaffe, W. R. Cook, and H. Jaffe, *Piezoelectric Ceramics* (Academic, London, 1971), p. 136.
[4] S. F. Liu, S-E. Park, T. R. Shrout, and L. E. Cross, J. Appl. Phys. **85**, 2810 (1999).
[5] B. Noheda, D. E. Cox, G. Shirane, J. A. Gonzalo, L. E. Cross, and S.-E. Park, Appl. Phys. Lett. **74**, 2059 (1999).
[6] B. Noheda, J. A. Gonzalo, L. E. Cross, R. Guo, S.-E. Park, D. E. Cox, and G. Shirane, Phys. Rev. B **61**, 8687 (2000).
[7] B. Noheda, D. E. Cox, G. Shirane, R. Guo, B. Jones, and L. E. Cross, Phys. Rev. B **63**, 014103 (2000).
[8] B. Noheda, D. E. Cox, G. Shirane, S. E. Park, L. E. Cross, and Z. Zhong, Phys. Rev. Lett. **86**, 3891 (2001).
[9] D. La-Orauttapong, B. Noheda, Z. G. Ye, P. M. Gehring, J. Toulouse, D. E. Cox, and G. Shirane, Phys. Rev. B **65**, 144101 (2002).
[10] B. Noheda, Z. Zhong, D. E. Cox, G. Shirane, S. E. Park, and P. Rehrig, Phys. Rev. B **65**, 224101 (2002).
[11] K. Ohwada, K. Hirota, P. W. Rehrig, Y. Fujii, and G. Shirane, Phys. Rev. B **67**, 094111 (2003).
[12] J. M. Kiat, Y. Uesu, B. Dkhil, M. Matsuda, C. Malibert, and G. Calvarin, Phys. Rev. B **65**, 064106 (2002).
[13] Z. G. Ye, B. Noheda, M. Dong, D. Cox, and G. Shirane, Phys. Rev. B **64**, 184114 (2001).
[14] B. Noheda, D. E. Cox, G. Shirane, J. Gao, and Z. G. Ye, Phys. Rev. B **66**, 054104 (2002).
[15] F. Bai, N. Wang, J. Li, D. Viehland, P. Gehring, G. Xu, and G. Shirane, J. Appl. Phys. **96**, 1620 (2004).
[16] H. Fu and R. E. Cohen, Nature (London) **403**, 281 (2000).
[17] D. Vanderbilt and M. H. Cohen, Phys. Rev. B **63**, 094108 (2001).
[18] S. Wada, S. Suzuki, T. Noma, T. Suzuki, M. Osada, M. Kakihana, S. Park, L. E. Cross, and T. Shrout, Jpn. J. Appl. Phys., Part 1 **38**, 5505 (1999).
[19] Y. Lu, D.-Y. Jeong, Z.-Y. Cheng, Q. M. Zhang, H. Luo, Z. Yin, and D. Viehland, Appl. Phys. Lett. **78**, 3109 (2001).
[20] Y. Guo, H. Luo, T. He, H. Xu, and Z. Yin, Jpn. J. Appl. Phys., Part 1 **41**, 1451 (2002).
[21] D. Viehland and J. F. Li, J. Appl. Phys. **92**, 7690 (2002).
[22] F. Jona and G. Shirane, *Ferroelectric Crystals* (Pergamon Press, New York, 1962).